EnvironmentAsia
The international journal by the Thai Society of Higher Education Institutes on Environment

EnvironmentAsia 18(2) 2025 1-15
DOI 10.14456/ea.2025.31
ISSN 1906-1714; ONLINE ISSN: 2586-8861

Biosorption Potential of Modified Guava *(Psidium guajava)* Leaf adsorbent for Sustainable Adsorption of Heavy Metals

Harshala Kasalkar[1], Namrata Kislay[1], Asmita Jadhav[2], Nilesh Wagh[2], and Geeta Malbhage[1*]

[1]*Amity School of Applied Sciences, Amity University, Mumbai, Maharashtra-410206, India*
[2]*Department of Environment Science, Somaiya Vidyavihar University, Mumbai 400077, India*

*Corresponding author: gkmalbhage@mum.amity.edu
Received: December 6, 2024; Revised: February 13, 2025; Accepted: March 21, 2025

Abstract

The application of novel biomass materials has gained attention for the removal of hazardous pollutants in the last decades. The waste derived adsorbent was rigorously studied over the conventional chemical adsorbents. Accordingly, modified guava (*Psidium guajava*) leaves (MGLP) were used in this study as a biosorbent to remove lead (Pb) and chromium (Cr) from aqueous solutions. The surface properties of modified guava leaves adsorbent were studied using techniques including FTIR, pXRD, FESEM, and BET surface area measurements. Batch experiments were conducted to evaluate dose optimization, adsorbent size, adsorbent behaviour, pH kinetics and isotherms. The adsorption parameters were calculated for MGLP. The Langmuir model described the monolayer adsorption mechanism with a maximum adsorption capacity of 47.62 mg/g and 54.34 mg/g for Pb (II) and Cr (VI), respectively, with the adsorption kinetics following a pseudo-second order pattern. pH experiments indicate the broad applicability of MGPL for Pb (II) and Cr (VI) removal across pH range 2-8. These results highlighted MGLP as a cost-effective, biomaterial-based adsorbent for wastewater treatment applications.

Keywords: Biosorbent; Plant waste; *Psidium guajava*; Sustainability; Adsorption

1. Introduction

Environmental contamination of natural resources is a big concern for scientists throughout the world. Heavy metals contamination of water resources poses a serious risk to all forms of life, including humans. Even trace levels of heavy metals in groundwater and freshwater resources render these resources unsuitable for utilization in various purposes. According to the United Nations Sustainable Development Goals Report (2023), 2.2 billion people around the world still need safely managed drinking water in 2022. Along with 703 million people, who are still lacking water for their basic needs (The SDG Report, 2023). The scientific community, locally as well as internationally, highlights the requirement for continuous research to combat the occurrence of heavy metals contamination in water resources. The anthropogenic contamination of heavy metals such as chromium (Cr), lead (Pb), mercury (Hg), arsenic (As), cadmium (Cd) through various industries and household activities pollutes water resources (Bayuo *et al.,* 2020).

The widespread environmental impact of these heavy metals through different pathways can lead to toxicity to humans and other animals. Pb (II) and Cr (VI) contamination of aquatic environments include both anthropogenic and natural sources. The anthropogenic contamination of chromium occurs through the discharges of electroplating, dye production, paint, tannery, chemicals, wood preservation, petroleum, and alloy manufacturing industries (Zhitkovich, 2011; Kerur *et al.,* 2020). In the United States of America (USA), a major contributor to the anthropogenic contamination of chromium in drinking water is the cooling tower discharge containing toxic Cr (IV), sources of lead (Pb) contamination include discharges from lead batteries, lead paints, PVC pipes used for sanitation, agricultural purposes, mining discharges. (Singh *et al.,* 2022). Lead (Pb) contamination of drinking water resources mainly occurs through corrosion of lead- containing plumbing materials due to highly acidic or low mineral- containing water (EPA, 2016). Cr (VI) and Pb (II) are potentially hazardous chemicals recognized for their irreversible toxic effect on living organisms and the environment. (Zhitkovich, 2011; Rahman and Singh, 2019). Excessive exposure to Cr (VI) ions leads to severe diarrhea, vomiting, nausea, epigastric pain, and hemorrhaging. The toxicity of chromium leads to nephrotoxic, mutagenic, and carcinogenic effects. Highly reactive nature of Cr (VI) ions compelled them to attached weekly to inorganic surfaces. (Shijie Xie, 2024) Lead (Pb) toxicity also results in abdominal pain, and mainly affects respiratory systems causing disease, such as lung cancer, chronic obstructive pulmonary disease (COPD), and asthma. It also damages kidneys, nervous system, and the cardiovascular system (Raj & Das, 2023).

The World Health Organization (WHO) guidelines set the maximum acceptable limit for Cr (VI) in drinking water at 0.05 mg/L and for Pb (II) at 0.01 mg/L (EPA, 2016; Leonard *et al.,* 2023). Hence, research organizations throughout the world are engaged to find sustainable technologies for these pollutants to meet the guidelines. Various treatment techniques have been reported for removing pollutants like chromium and lead from waste water: physical methods, chemical methods, biological methods, membrane-based technologies, electrochemical methods, etc. (Kerur *et al.,* 2020; Raj and Das, 2023; Leonard *et al.,* 2023). Among these methods, physical methods are widely used, including adsorption methods. This method has gained attention from technologists and researchers due to their merits such as, efficiency to ppb level, cost-effectiveness, and low operating and maintenance charges (Leonard *et al.,* 2023). Various types of adsorbents, like inorganic metal oxide-based, organic, MOF, biosorbents, etc. Metal-based adsorbents have problems like metal leaching and toxicity (Oliveira *et al.,* 2008], which is why researchers are now more interested in biosorbents. Hence, the synthesis of economical biosorbents gained attention for the development of cost-effective technologies for the elimination of heavy metals from water and wastewaters (Oliveira *et al.,* 2008; Bayuo *et al.,* 2020; Kerur *et al.,* 2020).

The biosorbents which are reported in recent decades include agricultural waste as well as industrial waste materials like coffee husk, rice husk, fly ash, sawdust, groundnut husk, etc. (Oliveira *et al.,* 2008; Kerur *et al.,* 2020) There are some limitations, such as selection of potential precursors for the development of biosorbents, raw materials availability, reusability, etc. (Oliveira *et al.,* 2008).

Agricultural waste generation is inevitable, but instead of burning it and emitting tons of greenhouse gases, we should use it for economic purposes. In 2022, Castaneda-Figueredo et al. said that the peels of oranges, passion fruits, and potatoes could be used as adsorbents to get rid of lead and chromium from metal solutions. Balaji *et al.* (2014) wrote about a study that used *Arthrospira* (spirulina) species as biosorbents to remove cadmium, lead, and chromium. Singh *et al.* in 2024, looked into how *Arachis hypogaea* (groundnut) husk can be heated and turned into biochar. They then used biochar to remove Cr (VI) from water. In 2023, Abdullah and Othman looked into how activated carbon made from guava leaves could remove Methylene Blue from solutions by studying its adsorption and physiochemical properties. In the past decades, researchers have focused on biosorbents, although they have some limitations, like low surface area, availability, and efficiency. However, their cost efficiency in comparison to conventional adsorbents identifies them as significant candidates (Argun *et al.,* 2007).

Psidium guajava, commonly known as Guava, is a medicinal plant that belongs to the Myrtaceae family (Mitra & Das, 2019). In addition to their therapeutic potential, guava leaves have been associated with the adsorption of heavy metals, including cadmium, zinc, arsenic, iron, lead, and chromium, as well as various dyes such as brilliant green, methylene blue, congo red, nile blue, auramine, amaranth, and photocatalytic dyes from polluted water sources, due to their porous structure and functional groups. (Ali *et al.,* 2022; Dey *et al.,* 2022; Dey *et al.,* 2023; Mustafa *et al.,* 2023; Mohapatra *et al.,* 2024; Chanda *et al.,* 2025). The literature pool comprises all studies examining guava plant leaf as biosorbents over the last decade.

Although this plant is indigenous to Central America, it is extensively farmed in many countries, including tropics, subtropics, and Mediterranean areas (Argun *et al.,* 2007; Mitra & Das, 2019; Abdullah & Othman, 2023). India, being a major cultivator of guava, generates significant quantities of guava leaves, especially fallen leaves which can be utilized for economical purposes in adsorbent development. So, this study focuses on using modified guava leaf powder (MGLP) as an adsorbent to remove chromium and lead from water-based metal solutions. The innovativeness of this study lies in its systematic exploration of the morphological transformations of plant leaf biosorbents, a gap previously unaddressed in the literature. Unlike prior works that focus primarily on adsorption efficiency, this study uniquely integrates morphological assessments using pXRD, FTIR, FESEM, and BET surface area analysis to understand the impact of mild alkali modification on guava leaf powder (MGLP). The research also provides novel insights into the role of particle size in adsorption behaviour, contributing to a deeper understanding of biosorption mechanisms. The high adsorption efficiency of MGLP for Pb (II) and Cr (VI), adherence to the Langmuir model, and performance across a wide pH range (2-8) highlight its practical applicability. By utilizing agricultural waste for heavy metal remediation, this study not only proposes an environmentally sustainable solution but also emphasizes the integration of technological and environmental assessments for effective decision-making in wastewater management.

The primary aim of this study was to assess the effectiveness of guava leaves for simultaneous adsorption of chromium and lead with different parameters. The primary objectives set to execute the study were: 1) to evaluate factors such as adsorbent particle size, pH, initial metal ion concentration, and adsorption kinetics; 2) to analyse the reaction rate to comprehend the adsorption mechanism. Second objective was to analyse modifications and pollutant loading effects on the biosorbents using surface characterization techniques like pXRD, FTIR, FESEM, and BET surface area measurements. It was also looked at how competing anions affect the adsorbent and its ability to regenerate in order to see if it could be used in real-life wastewater treatment. The application of modified guava (*Psidium guajava*) leaf as a waste biomass explored its potential as bioremediation technique for heavy metals that can reduce reliance on synthetic adsorbent promoting sustainable development. The study addresses a knowledge gap by systematically investigating morphological changes in plant leaf-derived biosorbents over time, a factor unexplored in prior literature, and demonstrates MGLP's significant adsorption capacities for Pb (II) and Cr (VI) across a wide pH range (2-8), underscoring its versatility for real-world wastewater treatment applications.

2. Methodology

2.1 Materials

Sodium Hydroxide pellets (NaOH) (Merck, Supelco, ACS reagent grade) were utilized for adsorbent modification. Standard stock solutions of metal salts of Pb (II) and Cr (VI) (Inorganic Ventures, USA,1000 ug/mL each), were dissolved in deionized water (Milli-Q) to prepare stock solutions for adsorption investigations. Nitric acid (HNO_3) (Merck, Supelco, ACS reagent), Hydrochloric acid (HCl) (Merck, ACS reagent, Supelco Hydrochloric acid fuming 37%,) and Sodium Hydroxide pellets (NaOH) (Merck, Supelco, ACS reagent grade) were used to prepare solution for pHpzc and pH experiments.

Sodium nitrate ($NaNO_3$), sodium chloride (NaCl) and sodium sulfate (Na_2SO_4) were obtained from Merck Millipore Limited and utilized without further purification for the co-anion study.

2.2 Preparation of modified guava leaf powder (MGLP) adsorbent

The fallen dried leaves of the guava plant were collected from the nearby Amity University area, Navi Mumbai, India. The collected leaves were washed with deionized water (18 MΩ resistivity, obtained from the Milli-Q DI water system), to remove dust particles and impurities. The leaves were then oven-dried at 80 ºC for 8 hours, crushed to powder, and sieved to get particle fractions ranging from 75 to 150 µm. The guava leaf powder was modified in the first step by treating it with sodium hydroxide (NaOH). An adequate amount of NaOH (Aftab *et al.*, 2024) was dissolved in water to achieve a final concentration of 5% NaOH in the modified adsorbent (with an excess of 10%). The required amount of guava leaf powder (25 g) was treated with the NaOH solution and stirred for 8hours. The resultant powder was then rinsed with deionized water and oven dried at 80 ºC for 8 hours. In the second step, the oven-dried material was cooled to room temperature and stored for further experiments.

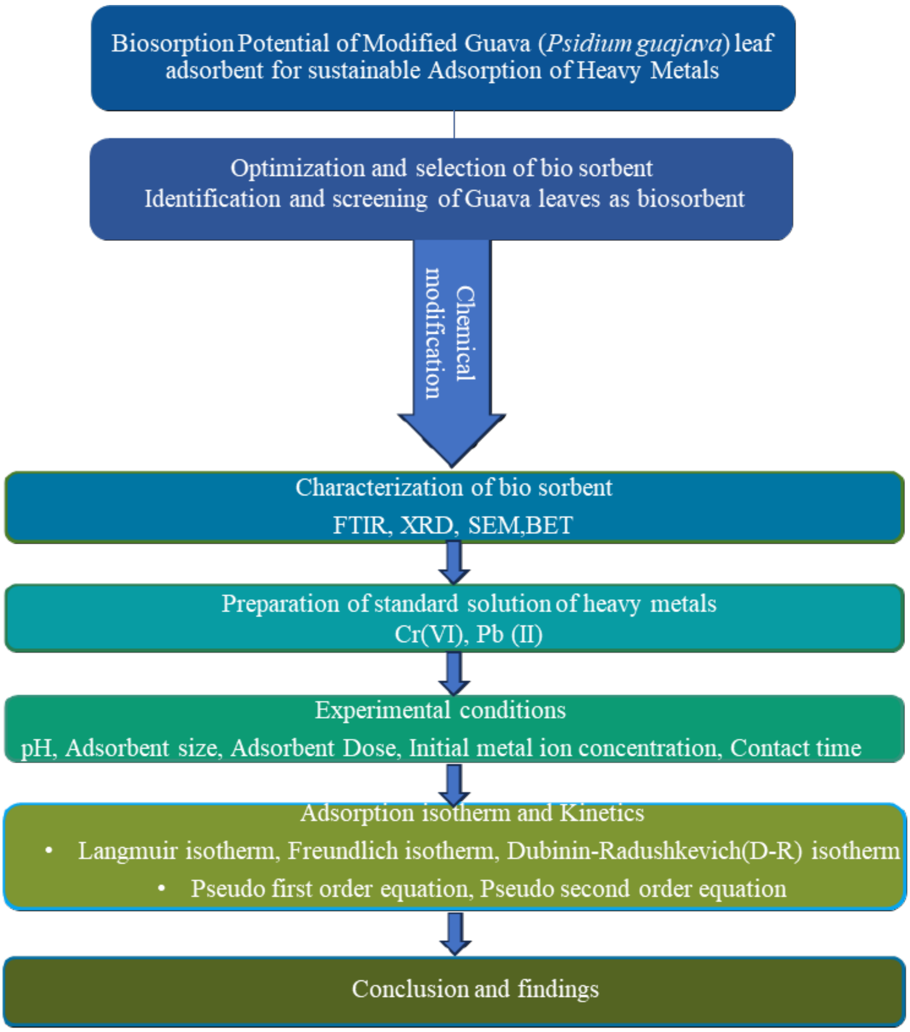

Figure 1. Representation of methodology opted for study

2.3 Adsorbent characterization

X-ray diffraction (XRD) characterization of the synthesized adsorbent was performed by using X-ray diffractometer (Benchtop, model-Rigaku Mini flex, Japan) employing Ni- filtered Cu Kα radiation (λ = 1.54 Å) at 15 mA and 30 kV. XRD patterns of the powered adsorbents were recorded in the 2θ range of 10 - 90º with a steps size of 0.02º per second. The generated biosorbent was subjected to FTIR (Fourier transform infrared) analysis using an FTIR spectrophotometer (FTIR: AGILENT CARY 630 WITH ATR & DIAL PATH) within the wave range of 4000-400/cm at 4/cm resolution. A field emission scanning electron microscope (FESEM, model Zeiss Ultra 55) was utilized to capture micrographs at 5 kV accelerating voltages. The specific surface area of MGLP was calculated using the nitrogen adsorption isotherm technique and a Micropore analyzer (ASAP 2020, Micromeritics, U.S.A.). The point of zero charge of the samples at different pH values (ranging from 2 to 12) was determined using NanoBrook Zeta PALS model.

2.4 Lead (II) and Chromium (VI) Adsorption Experiments

Modified guava leaf powder (MGLP) was employed as an adsorbent to study the uptake of Pb (II) and Cr (VI) ions in aqueous solutions. Batch studies were conducted to investigate the effect of several parameters including adsorbent size, biosorbent dose, Pb (II) and Cr (VI) ions concentration, contact time, pH, and competing anions. ICP-MS was used to detect Pb (II) and Cr (VI) ions in aqueous solutions calibrated with high purity standards. For each experiment, a predefined dosage of MGPL was added to 250 ml polypropylene flask containing 100 ml of synthetic Pb (II) and Cr (VI) aqueous solutions. The flasks were shaken at 150 ± 5 rpm in a rotary shaker (Remi India) at room temperature (30 ºC ± 2 ºC). The residual concentration of Cr (VI) and Pb (II) were analyzed after withdrawing samples from the experimental solutions at predetermined time intervals. The effect of the size of the adsorbent was evaluated to select the final adsorbent for detailed experiments. Dose optimization was performed to determine the optimal adsorbent required for efficient removal of Pb (II) and Cr (VI) ions from aqueous solutions. Adsorption kinetics were investigated by varying the initial metal (Cr (VI) and Pb (II)) ion concentrations and contact time. Biosorbent dose optimization was performed with Pb (II) and Cr (VI) concentrations in the range of 10 - 30 mg/L. Samples for the batch kinetic research were taken out at intervals of 20 to 180 minutes. The effect of pH on Pb (II) and Cr (VI) removal was evaluated by varying the pH from 2 to 11. The pH of the solution was adjusted by adding 0.1M NaOH and 0.1M HNO_3 solutions. Blank experiments (without the addition of absorbent) were conducted to account for any changes in metal ion concentration due to factors other than adsorption. All collected samples were filtered using disposable membrane filters with a pore size of 0.22 μm. The filtered water samples were analyzed using ICP-MS (Agilent Technologies, 7800 ICP-MS).

2.5 Data analysis

The equilibrium data for adsorption were fitted with different linear forms of isotherm models by modelling with MS Excel and Origin pro-2025. Experimental data is analysed using adsorption isotherm equations, Isotherm constants are determined and coefficient of correlation is calculated. The linear fit of the experimental data allows to obtain the value of correlation coefficient.

3. Results and Discussion

3.1 Biosorbent (MGLP) Characterization

The peaks observed in Figure 2 (a) at 16º, and 30º, indicating the presence of whewellite, (syn $C_2CaO_4.H_2O$). Whereas the peaks observed at 20º and 26º suggest the presence of quartz (Krishnani *et al.,* 2021). Whewellite is calcium oxalate monohydrate occurring naturally alongside the dihydrate form, weddellite, which is the less stable and most pervasive (Stephens WE, 2012; Krishnani *et al.,* 2021). Krishnani *et al.* (2021)

reported similar observations for the guava leaves modified absorbent. The presence of whewellite is proven in foliage and leaves with the XRD of reference materials like about 4.1% in tomato leaves, 3.7% in spinach, and 4.3% in peach leaves (Stephens WE, 2012). This phytochemical plays a significant role in the regulation of Ca^{2+} ion concentration, which is essential for plant survival under dry and abiotic stress conditions.

FTIR analysis gives important information on the surface functional groups of adsorbents. The IR spectra of MGLP adsorbent from Figure 2 (b) depict the band at 2920 cm^{-1} can be assigned to the aliphatic C-H stretching vibration (Behera *et al.,* 2021). Similarly, the presence of a weak broad band near 3289 cm^{-1} indicates O-H vibrations due to intermolecular H bonds in the cellulose and 1647cm^{-1} C=C stretch vibrations (Castañeda-Figueredo *et al.,* 2022). There was a band from 1647 cm-1 attributed to vibration of water molecules absorbed in the biopolymer, like cellulose. The IR spectra indicated that mild alkali, such as NaOH, has not altered the bands as the modified adsorbent is rich in cellulose. The complex nature of FTIR can be understood by the structural composition of plant-based

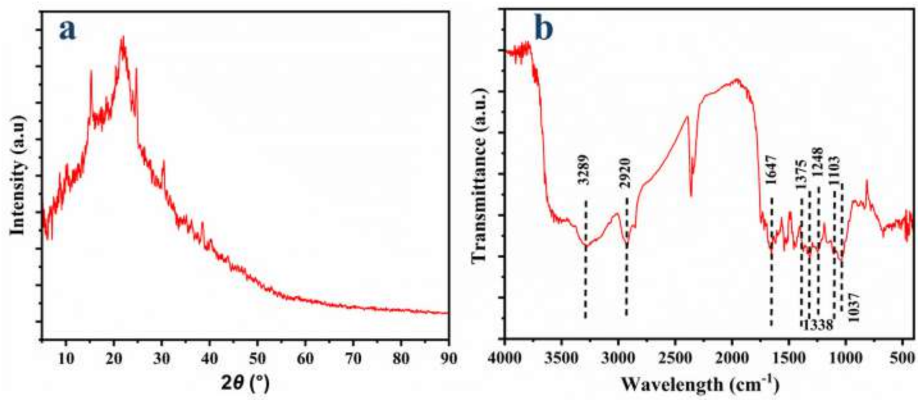

Figure 2. (a) pXRD and (b) FTIR of Modified guava leaf powder (MGLP) adsorbent

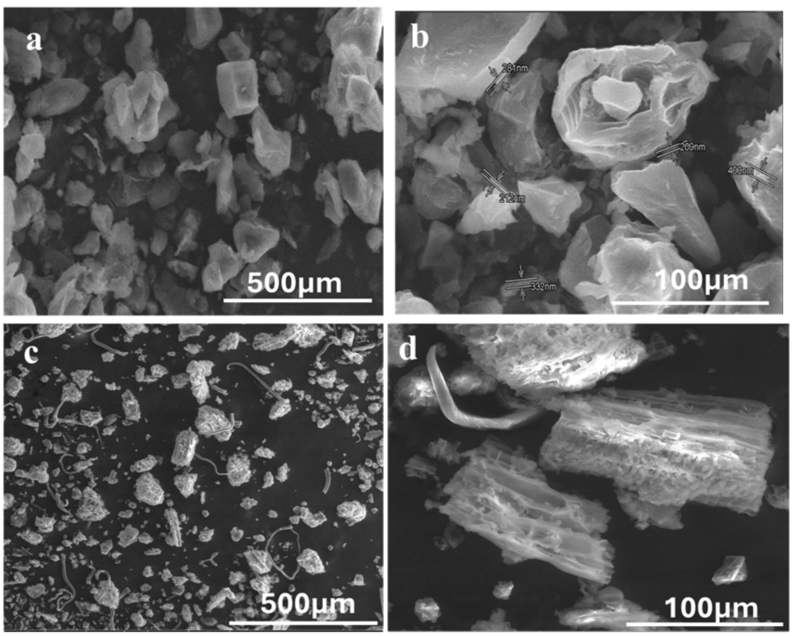

Figure 3. (a) and (b) FESEM of Modified guava leaf powder (MGLP) adsorbent before adsorption and (c), (d) after adsorption

materials due to the presence of cellulose, hemicellulose, sugars, pectin, and lignin, indicating the IR bands from 3300 cm^{-1} - 990cm^{-1} (Castañeda-Figueredo *et al.,* 2022). Based on the observation, the presence of hydroxyl, carbonyl, and C=C groups provide active sites for the adsorption of metal ions after modification of guava leaves.

The FESEM micrographs of the MGLP adsorbent are depicted in Figure 3 (a) and (b) shows a heterogenous surface with varying morphologies along with Figure 3 (c) and (d) after adsorption. The modifications observed due to alkali treatment showed microporous structures with less ordered morphologies. The BET Surface area of the untreated guava leaves and modified guava leaves powder was found to be 7.82 m^2/g and 98.24 m^2/g, respectively.

3.3 Batch adsorption Study

The adsorption characteristics of MGLP were studied through batch adsorption experiments under different experimental conditions. MGLP adsorbent was studied for different adsorption parameters, including size of the adsorbent, varying metal ion concentration, kinetics, and adsorption isotherm studies.

3.3.1 Effect of Size of MGLP

The effect of adsorbent size on the removal efficiency of Pb and Cr ion removal is shown in Figure 4 for the selection of the best particle size adsorbent for further analysis. As the adsorbent size plays a key role in determining the adsorption efficiency. Henceforth, the experiments were performed with initial Pb (II) and Cr (VI) ion concentrations as of 30 mg/L, at RT 30 ºC, 150 rpm, an adsorbent dose of 10 g/L, and varying sizes of 75 µm, 90 µm, and 150 µm for 120 min. Adsorption efficiency depends on the available surface of the adsorbent. The results showed that a particle size of 75 µm removed approximately 90% of the Pb (II) while, more than 99% removal of Cr (VI) was achieved. Regarding the Pb (II) ions, removal results indicate significant differences with size variation of the adsorbent. However, comparatively for Cr (VI) ion removal, there is no significant effect of particle size, as the 90 µm and 150 µm size adsorbents also showed more than 98% removal efficiency. Similar observations are reported by Ponnusami *et al.* (2008) to study the effect of Psidium guajava leaf powder in removing methylene blue from aqueous solutions as the smaller size particles have higher adsorption efficiencies. Based on these observations, the MGLP adsorbent with a particle size of 75 µm was selected for further experiments.

3.3.2 Effect of MGLP dosages

The results of adsorption tests using MGLP adsorbent with different starting amounts of Pb (II) and Cr (VI) are shown in Figure 5. Adsorbent doses were 2, 5, 10, and 20 g/L, with a contact time of 3 hours.

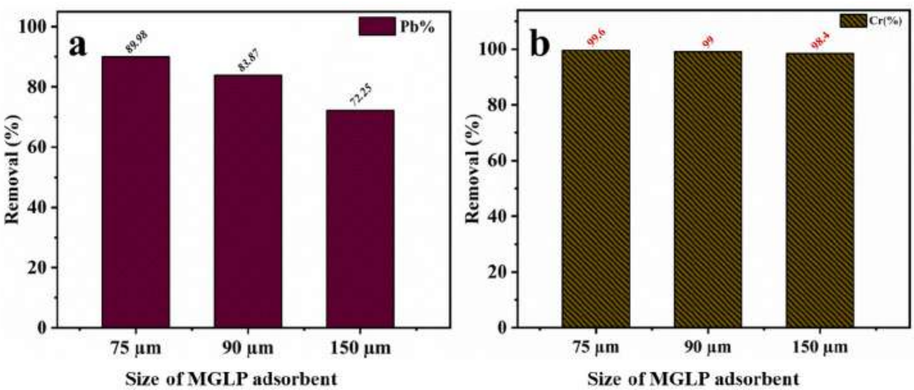

Figure 4. (a) and 3(b) Effect of size of MGLP adsorbent for the uptake of Pb (II) and Cr (VI) removal from water

It shows that, a dose of 2 g/L with initial Cr (VI) concentrations of 5, 10, 20, and 30 mg/L, resulted in ~ 99% removal. However, with similar experimental conditions for Pb (II) observed that with doses of 2, 5, 10, and 20 g/L removal efficiency was found to be 90.36%, 86.78%, 85.07, and 84.61% respectively. A dose of 5 g/L was found to be efficient for both Pb (II) and Cr (VI)as shown in Figure 5 b. This dose was able to remove the initial Pb (II) concentration of 5, 10, 20 and 30 mg/L to 96.89%, 95.54%, 92.05%, and 88.48% with the reaction time of 3hours. Figure 5 c shows results with adsorbent dose of 10 mg/L, this dose showed maximum removal efficiency as ~ 83.9% with 30 mg/L initial Pb (II) concentration. As shown in Figure 5 d, for high adsorbent dose of MGLP as 20 mg/L removal efficiency reduced for Cr (VI). However, in the case of Pb (II), it was observed that there is a slight increase in the removal efficiency. From the comparative analysis of the MGLP adsorbent dose study, it is evident that with the increasing concentration, efficiency was reduced. However, the high amount of adsorbent is not efficient as it may lead to saturation of adsorbent sites leading to the efficiency reduction. Hence based on the findings, the adsorbent dose of 5 g/L was selected for kinetics, isotherms, pH and other studies.

3.3.3 Effect of contact time

The results of the adsorption kinetics of the MGLP adsorbent with different initial concentrations of Pb (II) and Cr (VI) as 10, 20, and 30 mg/L with a defined dose of 5 g/L are represented in Fig.6 (a and b). Precisely, for initial Cr (VI) concentrations of 10, 20, and 30 mg/L, at 30 min the removal efficiency was 97.9, 97.8, and 98.4%, respectively. Fig. 6 a reveals that the dose of 5 g/L was efficient to eliminate ~ 90% of the Cr (VI) ions within the initial 20 minutes of the process, with equilibrium attained within the first 30 minutes. Figure 6 b showed that the dose of 5 g/L was effective to achieve ~ 75% removal of Pb (II) within the first 20 min of the reaction. The initial 10 mg/L of Pb (II)

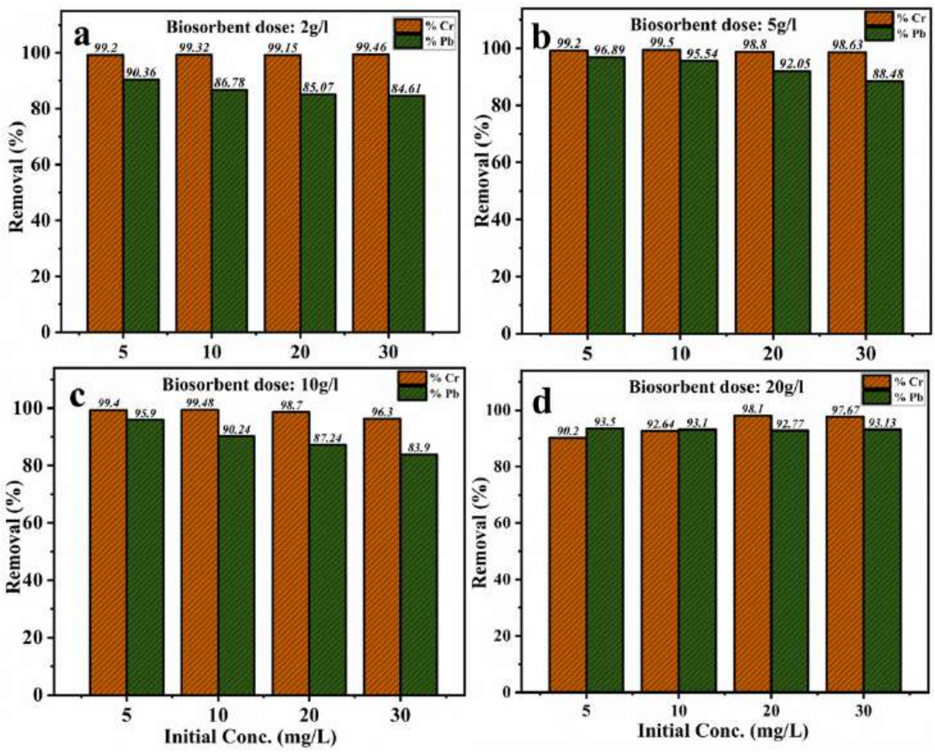

Figure 5. Results of biosorbent dose and adsorption obtained from MGLP (a, b, c, d) at various initial Cr (VI) and Pb (II) concentrations, at different dose as 2, 5, 10, 20g/L and 3hours contact time

concentration was reduced to > 80% within first 10 min of the reaction, then the equilibrium achieved after 30 min and as the Pb (II) concentrations increased removal efficiency decreased. After 30 min, i.e. the second stage of the reaction, saturation was observed, a few Pb (II) and Cr (VI) ions may be adsorbed on the surface. In the first half of the reaction, the ions of Pb (II) and Cr (VI) quickly occupies the adsorbent sites till the available sites reduce. Figure 6 clearly shows that for different initial concentrations of both Pb (II) and Cr (VI), more than~75% removal occurred within the first 20 minutes, showing prompt uptake. However, with the increasing concentration, the contact time required to achieve equilibrium increases. Researchers observed that the second stage generally, the high concentration of metal ions, forces to the ion exchange mechanism that is a comparatively slow adsorption phenomenon (Jadhav *et al.,* 2020).

3.3.4 Effect of pH

The results of the pH adsorption study of the MGLP adsorbent are described in Figure 7. pH adsorption experiments are very important for understanding the field applications of any adsorbent. Therefore, to understand the behavior of MGLP adsorbent under different acidic and alkaline conditions, a set of experiments was conducted at room temperature (30 ºC) with initial concentrations of Pb (II) and Cr (VI) as 10 mg/L, with a dose of 5 g/L with a reaction time of 3 hours. The solution pH was maintained by using 0.1M HCl and 0.1M NaOH solutions. As it is evident from Figure 7, pH 4 and pH 6 showed maximum removal efficiencies as 98.5% and 99% for Cr (VI) removal and 96.28% and 98.21% for Pb (II) ions from water, respectively. Pb (II) and Cr (VI) removal efficiency was reduced with the change in pH of the solution from pH 2 to pH 9. The Pb (II) and Cr (VI) removal efficiency reduced to 88.71% and 89.2%, respectively. From the current study, it is stated that the point of zero charge (pzc) of the guava leaves powder is approximately around ~ 6.8, and after NaOH treatment, it was observed to be 7.2. Hence when solution pH is below pzc value the adsorption occurs whereas after pzc the adsorption sites are not available leading to reduced efficiency of metal ions (Abdullah & Othman, 2023).

3.3.5 Adsorption Isotherms and Kinetics:

Adsorbent experiments were conducted to determine the adsorption potential and characteristics of the adsorbent of the MGLP adsorbent. Figure 8a, 8b and 8c shows the results of Langmuir Freundlich and Dubinin-Radushkevich (D-R) adsorption isotherm of MGLP adsorbent to the uptake of Pb (II) and Cr (VI)from water. (Rajahmundry *et al.,* 2021) The mathematical expression for the Langmuir adsorption isotherm (linear form) is given by equation 1.

$$\frac{1}{q_e} = \frac{1}{q_m KLC_e} + \frac{1}{q_m} \qquad (1)$$

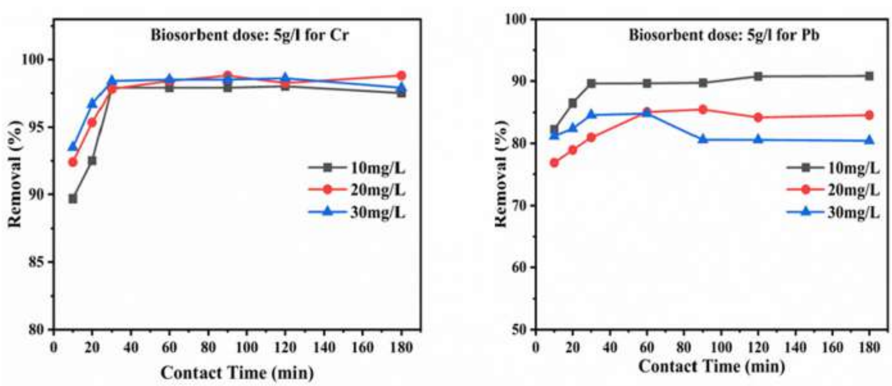

Figure 6. Adsorption kinetic results data obtained from MGLP at different concentrations Cr (VI), Pb (II) (a, b) (10, 20 and 30 mg/L and dose 5 g/L)

where, q_e and C_e represents the amount of adsorbed metal ions Pb (II) and Cr (VI) per unit mass of the MGLP adsorbents and the concentration of metal ions Pb (II) and Cr (VI) remaining in the solution (mg/L) at the equilibrium and q_m denotes maximum adsorption capability of the adsorbent, respectively. Whereas K_L (L/mg) expresses the constant of Langmuir equilibrium.

The Freundlich adsorption model may be represented as follows (Freundlich, 1907):

$$Ln(q_e)=\ln k_f + 1/n \ln (C_e). \quad (2)$$

where q_e signifies the adsorbate adsorbed at equilibrium per unit weight of adsorbent (mg/g), q_m denotes the maximum adsorption capacity (mg/g), and C_e denotes the equilibrium concentration of adsorbate in solution (mg/L).

The Dubinin-Radushkevich (D-R) adsorption model is represented as follows (Dubinin, 1960)

$$q_e = q_{max}\, e^{-\beta\varepsilon} \quad (3)$$

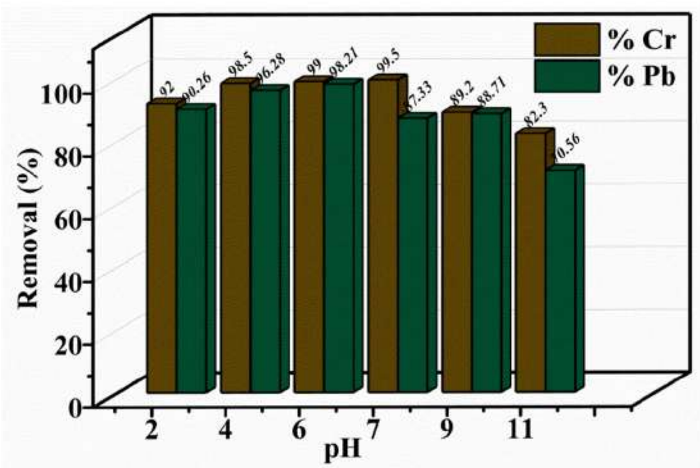

Figure 7. pH-adsorption study of MGLP adsorbent of Pb (II) and Cr (VI) uptake from water at 10 mg/L concentration and 5 g/L adsorbent dose

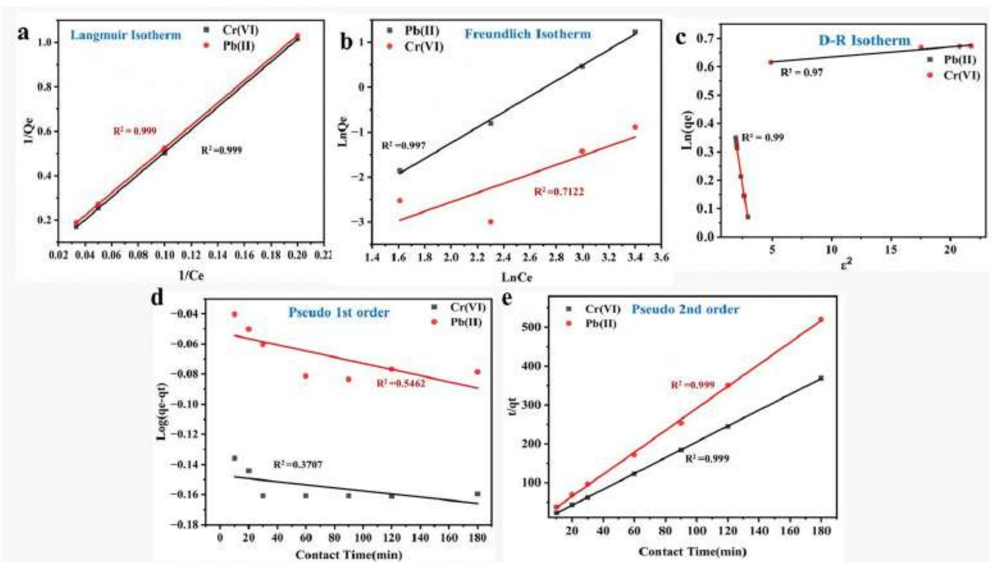

Figure 8. Adsorption isotherm: Langmuir isotherm (a), Freundlich isotherm (b) Dubinin-Radushkevich (D-R) isotherm (c) (Fitted by linear regression) and Pseudo first-order kinetic model (d) Pseudo second-order (e) kinetic model of Cr (VI) & Pb (II) uptake of metal ions on the surface of MGLP adsorbent.

where, q_e stands for the sorbed amount (mg/g); q_{max} is Dubinin Kagaber Radushkevich (DKR) monolayer capacity, ε is Polanyi potential, and β denotes the activity coefficient related to mean sorption energy (KJ/mol).

The regressed parameters are shown in Table 1. The calculated maximum adsorption capacities from the Langmuir model were 54.34 mg/g and 47.62 mg/g for Pb (II) and Cr (VI), respectively and correlation coefficients (R^2 =0.999) indicate that the Langmuir adsorption model is best suited to describe the adsorption equilibrium for MGLP for Cr (VI) and Pb (II). The Langmuir adsorption isotherm shows the adsorption behaviour of MGLP, indicating monolayer adsorption. (Al-Ghouti & Da'ana, 2020)

In this study biosorption of heavy metals, correlation coefficients (R^2 = 0.999) obtained from statistical and modelling factors. The authors have used adsorption experimentation results as dataset, which is why the regression line may perfectly fit the data. Additionally, the multi-parameter analysis was carried out in this study. The coefficient of determination close to unity indicates the applicability of adsorption and kinetics models employed in the present study.

The Langmuir adsorption isotherm represents strong interactions between the biobased adsorbents and adsorbates, indicating the impact of initial metal ion concentrations and the high energy active sites occupied with increasing concentrations of metal ions. Hence, with low initial concentration, these adsorption sites tend to occupy lower-energy sites (Behera *et al.,* 2021; Castaneda-Figueredo *et al.,* 2022).

Adsorption kinetics of adsorbates Pb (II) and Cr (VI) adsorption by MGLP were also investigated. As shown in Figs. 8d. and 8e., pseudo-first-order and pseudo-second-order kinetic models are best accounted for the adsorption kinetic results obtained for Pb (II) and Cr (VI). Figure 8c presents the findings of the pseudo-firs-order kinetic model for the adsorption of Cr (VI) and Pb (II), with the linear representation of this model articulated through the Lagergren equation. (Eq.4) (Lagergren, 1898)

$$\log(Q_e - Q_t) = \log(Q_e) - K_1 . t \quad (4)$$

where, Q_t denotes the amount of adsorbate adsorbed at time t (mg/g), and Q_e represents the amount of adsorbate at equilibrium concentration. The equilibrium rate constant for a pseudo-first order reaction is K_1, and the rate constants are obtained by plotting log (Q_e–Q_t) against time (t). Table 2 provides information on the criteria for pseudo-first-order fits. The analysis reveals a significant lack of alignment in the correlation coefficients, indicating that the gathered data do not conform to the pseudo-first-order kinetic model. This suggests that the adsorption rate remains unaffected by the concentration of the adsorbate in the solution. (Lagergren, 1898)

Figure 8 d. expresses the outcomes of the pseudo-second-order kinetic model plotted as time (t) vs t/Q_t to ascertain the rate constant and Q_e values. This model is represented by Eq.(5) (Ho & McKay, 1999) as

$$\frac{t}{Q_t} = \frac{1}{K_2 Qe} + \frac{1}{Qe} . t \quad (5)$$

where, K_2 stands for the rate constant for pseudo-second-order adsorption expressed in g/ (mg min) units. K_2 and Q_e are determined by the intercept and slope of the t vs. t/Qt plot, respectively. Table 2 denotes the details of pseudo-second-order fitting parameters. With correlation coefficients near unity,

Table 1. Langmuir and Freundlich adsorption Isotherms characteristics of MGLP adsorbent to the uptake of Pb (II) and Cr (VI)from water

Langmuir Adsorption Isotherm			Freundlich Adsorption Isotherm			Dubinin-Radushkevich (D-R) Isotherm		
Parameter	Cr (VI)	Pb (II)	Parameter	Cr (VI)	Pb (II)	Parameter	Cr (VI)	Pb (II)
K_L	0.0042	0.0037	n	1.037	1.734	β	0.0043	3.57
$1/Q_m$	0.021	0.0184	In K	4.6	4.7	Q_m	1.79	23.57
Q_m	47.62	54.34	K_F	102.8	109.9	ε (KJ/mol)	0.528	0.146
R^2	0.999	0.999	R^2	0.7122	0.997	R^2	0.9527	0.9980

the pseudo-second-order model is suitable for the MGLP adsorbent kinetic data very well. This model posits that chemisorption serves as the adsorption mechanism, with the adsorption rate being dictated by the adsorption capacity rather than the adsorbate concentration. The results align well with existing literature, suggesting that the pseudo-second-order kinetic model is appropriate for the kinetic data of biomass-derived adsorbents. (Dubinin, 1960).

3.3.6 Comparison between adsorption capacity of MGLP and other adsorbents:

The adsorption capacity MGLP was compared with the recorded adsorbents for Pb (II) and Cr (VI) removal as shown in Table 3. In comparison with previous investigations, the MGLP adsorbent's maximum adsorption capacity is significantly more substantial. (Wang and Guo, 2020) The adsorbents dose necessary for effective adsorption, and the initial Pb (II) and Cr (VI) ions concentration used in the investigation are recorded in Table 3. As stated by this table, the biosorbent MGLP exhibits more effective Pb (II) and Cr (VI) adsorption than the other adsorbents that have been described, including nanocomposites and nano mixed metal oxides. (Bardestani *et al.,* 2019; Abatan *et al.,* 2020].

To summarize, the results demonstrated that, the MGLP adsorbent is a promising material for the remediation of Pb (II) and Cr (VI) from water and has potential for removal of other ions as well.

Table 2. Characteristic kinetics of Pseudo 1st order and Pseudo 2nd order models of MGLP adsorbent to the uptake of Pb (II) and Cr (VI) from water

Pseudo 1st order Isotherm			Pseudo 2nd order Isotherm		
Parameter	Cr (VI)	Pb (II)	Parameter	Cr (VI)	Pb (II)
R^2	0.3707	0.5462	R^2	0.9999	0.999
q_e	1.143	1.128	q_e	0.49	0.3457
K_1	0.003	0.006	K_2	1.87	0.356

Table 3. Uptake capacity of different adsorbents in comparison of Pb (II) and Cr (VI)

Adsorbent	Concentration (mg/L)	Dose (g/L)	Adsorption capacity (mg/g) for Cr (VI)	Adsorption capacity (mg/g) for Pb (II)	Reference
Cobalt ferrite-supported activated carbon	5	0.5	23.6	6.27	[Yahya *et al.,* 2020]
Bagasse fly ash	5-50	10	1.8	3.8	[Gupta &Ali 2004]
Biochar	5	1		7.9	[Bardestani *et al.,* 2019]
Fe3+/Fe2+ black cumin seeds (FNS)	-	-	15.75	19.99	[Thabede *et al,.* 2021]
Prestine Nigella Sativa seeds (PNS)	-	-	15.11	12.06	[Thabede *et al.,* 2021]
Eggshell	50	5	10.71	-	[Abatan *et al.,* 2020]
This study	5	10	47.62	54.34	Present study

4. Conclusion

In the present study, mild alkali-modified guava leaf powder (MGLP) was investigated as a biosorbent for understanding the uptake properties of Pb (II) and Cr (VI) from aqueous solutions. The surface properties of MGPL were analyzed using techniques such as pXRD, FTIR, FESEM, and BET surface area measurements. Preliminary experiment on the size of the adsorbent particle highlighted the importance of particle size in determining adsorption behavior. The adsorption parameters for the MGLP were calculated and the Langmuir model was found to explain the monolayer adsorption mechanism, with a maximum adsorption capacity of 54.34 mg/g for Pb (II) and 47.62 mg/g for Cr (VI); Correlation coefficients ($R^2 = 0.999$) demonstrated that the Langmuir adsorption model is most appropriate for describing the adsorption equilibrium of MGLP for Cr (VI) and Pb (II). The kinetics followed the pseudo-second-order model. pH experiments indicated the applicability for efficient removal of Pb (II) and Cr (VI) across pH range of 2-8. This study elucidates the potential of mild alkali-modified guava leaf powder (MGLP) as an effective biosorbent for removing Cr (VI) and Pb (II) from aqueous solution. It demonstrates the materials' high efficiency, fitting the Langmuir model with significant maximum adsorption capacities for both metals. It also proved suitable for diverse pH conditions (2-8) in wastewater treatment.

This investigation emphasizes the use of readily available agricultural waste like guava leaf as a promising adsorbent for the removal of heavy metals, thereby reducing environmental pollution. The investigation evaluates the capacity of MGLP, as an agricultural waste-based biosorbent, for the adsorption and immobilization of heavy metals, positioning it as a potential remediation technique. The study further highlights the potential of MGPL as a suitable and economically viable solution for heavy metal remediation, underscoring the importance of integrating technological and environmental assessments for inform decision-making in environmental management practices.

References

Abatan OG, Alaba PA, Oni BA. Performance of eggshells powder as an adsorbent for adsorption of hexavalent chromium and cadmium from wastewater. SN Applied Sciences 2020, 2: 1996

Abdullah MF and Othman NF, Physicochemical and adsorption properties of guava leaves-activated carbon by hydrochloric acid on adsorption of methylene blue. Scientific Research Journal 2023, Vol 20, No 1 33-49

Aftab RA, Yusuf M, Ahmad F. Green Technology Approach Towards the Removal of Heavy Metals, Dyes, and Phenols from Water Using Agro-based Adsorbents: A Review. Chemistry- an Asian Journal 2024; 19, e202400154

Al-Ghouti MA & Da'ana DA. Guidelines for the use and interpretation of adsorption isotherm models: A review. Journal of Hazardous Materials 2020; 393, 122383.

Argun ME, Dursun S, Ozdemir C, Karatas M. Heavy metal adsorption by modified oak sawdust: Thermodynamics and kinetics. Journal of Hazardous Materials 2007; 141:77–85

Ali AE, Mustafa AA, Eledkawy MA, Ahmed AM, Alnaggar GA, Elmelegy E, Kolkaila S. Removal of Cadmium (II) from Water by Adsorption on Natural Compound. Journal of Environmental Treatment Techniques 2022; 10(2), 164-169.

Behera US, Mishra PC, Radhika GB. Optimization of multiple parameters for adsorption of arsenic (III) from aqueous solution using Psidium guajava leaf powder. Water Science and Technology 2021; 85:515–34

Balaji S, Kalaivani T, Rajasekaran C, Shalini M, Siva R, Singh RK. Arthrospira (Spirulina) Species as Bioadsorbents for Lead, Chromium, and Cadmium a Comparative Study. CLEAN Soil Air Water 2014; 42:1790–7

Bardestani R, Roy C, Kaliaguine S. The effect of biochar mild air oxidation on the optimization of lead (II) adsorption from wastewater. Journal of Environmental Management 2019; 240:404–20

Bayuo J, Abukari MA, Pelig-Ba KB. Desorption of Lead (II) and Chromium (VI) ions and regeneration of the exhausted adsorbent. Applied Water science 2020; 10,171

Castañeda-Figueredo JS, Torralba-Dotor AI, Pérez-Rodríguez CC, Moreno-Bedoya AM, Mosquera-Vivas CS. Removal of lead and chromium from solution by organic peels: effect of particle size and bio-adsorbent. Heliyon 2022; 8: e10275

Chanda S, Kaliannan D, Balamuralikrishnan B, Shanmugam S, Rajendran S, Hesam K, Shreeshivadasan C. Process development of guava leaves with alkali in removal of zinc ions from synthetic wastewater, Journal of the Taiwan Institute of Chemical Engineers, 2025; Volume 166, Part 1,105283

Dey S, Kotaru NSA, Veerendra GTN, Sambangi A. The removal of iron from synthetic water by the applications of plants leaf biosorbents. Cleaner Engineering and Technology 9 2022; 100530

Dey S, Veerendra GTN, Phani Manoj AV, Anjaneya Babu PSS. Performances of plant leaf biosorbents for biosorption of phosphorous from synthetic water, Cleaner Materials 2023. Volume 8,100191

Dubinin MM. The potential theory of adsorption of gases and vapors for adsorbents with energetically non uniform surface. Chemical Reviews 1960; 60: 235–266

Environment Protection Agency, Basic Information about Lead in Drinking Water, (2016) Revised in Oct. 2024

Freundlich H, Ueber die Adsorption in Loesungen. Zeitschrift für Physikalische Chemie 1907; 57 385–470.

Gupta VK, Ali I. Removal of lead and chromium from wastewater using bagasse fly ash—a sugar industry waste. Journal of Colloid and Interface Science 2004; 271:321–328.

Jadhav AS, Ali Amrani M, Singh SK, Al-Fatesh AS, Bansiwal A, Srikanth VVSS. γ-FeOOH and γ-FeOOH decorated multi-layer graphene: Potential materials for selenium (VI) removal from water Journal of Water Process Engineering 2020; 37:101396.

Kerur S, Bandekar S, Hanagadakar MS, Nandi SS, Ratnamala GM, Hegde PG. Removal of hexavalent Chromium-Industry treated water and Wastewater: A review. Materials Today: Proceedings 2021;42: 1112–21

Krishnani KK, Choudhary K, Boddu VM, Moon DH, Meng X. Heavy metals biosorption mechanism of partially delignified products derived from mango (Mangifera indica) and guava (Psidium guajava) barks. Environmental Science and Pollution Research International 2021; 28:32891–904

Lagergren S. Zur theorie der sogenannten adsorption gelo¨ sterstoffe (About the theory of so–called adsorption of soluble substances), Kungliga Svenska Vetenskapsakademiens, Handlingar 1898; 24 1–39

Langmuir I. The adsorption of gases on plane surfaces of glass, mica and platinum, Journal of American Chemical Society 1918; 40, 1361–1403

Leonard J, Sivalingam S, Srinadh RV, Mishra S. Efficient removal of hexavalent chromium ions from simulated wastewater by functionalized anion exchange resin: Process optimization, isotherm and kinetic studies. Environmental Chemistry and Ecotoxicology 2023; 5:98–107

Mitra T, Das SK. Cr (VI) removal from aqueous solution using Psidium guajava leaves as green adsorbent: column studies. Applied Water Science 2019; 9,153

Mustafa AA, Ali AE, Kolkaila SA. Removal of Aluminum (III) from Water by Adsorption on the Sur-face of Natural Compound. Journal of Environmental Treatment Techniques 2023; 11(2), 88-93.

Oliveira WE, Franca AS, Oliveira LS, Rocha SD. Untreated coffee husks as biosorbents for the removal of heavy metals from aqueous solutions. Journal of Hazardous Materials 2008; 152:1073–81

Ponnusami V, Vikram S, Srivastava SN. Guava (Psidium guajava) leaf powder: Novel adsorbent for removal of methylene blue from aqueous solutions. Journal of Hazardous Materials 2008; 152:276–86

Rahman Z and Singh VP. The relative impact of toxic heavy metals (THMs) (arsenic (As), cadmium (Cd), chromium (Cr)(VI), mercury (Hg), and lead (Pb)) on the total environment: an overview. Environmental Monitoring and Assessment, (2019); 191(7).

Raj K, Das AP. Lead pollution: Impact on environment and human health and approach for a sustainable solution. Environmental Chemistry and Ecotoxicology 2023; 5:79–85.

Rajahmundry GK, Garlapati C, Kumar PS, Alwi RS & Vo DVN. Statistical analysis of adsorption isotherm models and its appropriate selection. Chemosphere 2021; 276, 130176

Singh K, Azad SK, Dave H. Effective removal of Cr (VI) ions from the aqueous solution by agro-waste-based biochar: an exploration of batch and column studies. Biomass Conversion and Biorefinery. 2024; 14, 19215–19229

Singh A, Sharma AK, Verma RL, Chopade RP, Pandit P, Nagar V. Heavy Metal Contamination of Water and Their Toxic Effect on Living Organisms. The Toxicity of Environmental Pollutants. intechopen.105075, 2022.

Shijie X. Water contamination due to hexavalent chromium and its health impacts: exploring green technology for Cr (VI) remediation, Green Chemistry Letters and Reviews 2024; 17:1, 2356614

Stephens WE, Whewellite and its key role in living systems. Geology Today 2012; 28:180–5

Thabede PM, Shooto ND, Xaba T, Naidoo EB. Magnetite Functionalized Nigella Sativa Seeds for the Uptake of Lead (II) and Chromium (VI)Ions from Synthetic Wastewater. Adsorption Science & Technology 2021.

The Sustainable Development Goals Report 2023: Special Edition a High-level Event Call to Action, United Nations publication issued by the Department of Economic and Social Affairs,2023

Ho YS, McKay G. Pseudo-second order model for sorption processes, Process Biochemistry. 1999; 34

Wang J & Guo X. Adsorption kinetic models: Physical meanings, applications, and solving methods. Journal of Hazardous Materials (2020); 390, 122156

Yahya MD, Obayomi KS, Abdulkadir MB, Iyaka YA, Olugbenga AG. Characterization of cobalt ferrite-supported activated carbon for removal of chromium and lead ions from tannery wastewater via adsorption equilibrium. Water Science and Engineering 2020; 13:202–13

Zhitkovich A. Chromium in Drinking Water: Sources, Metabolism, and Cancer Risks. Chemical Research in Toxicology 2011; 24:1617–29